

Narrating For You: Prompt-guided Audio-visual Narrating Face Generation Employing Multi-entangled Latent Space

Aashish Chandra K^{1*} Aashutosh A V^{1,2*} Abhijit Das^{1†}

¹Machine Intelligence Group, Department of CS&IS, BITS Pilani, Hyderabad Campus, India

²Georgia Institute of Technology, USA

abhijit.das@hyderabad.bits-pilani.ac.in

Abstract

We present a novel approach for generating realistic speaking and talking faces by synthesizing a person’s voice and facial movements from a static image, a voice profile, and a target text. The model encodes the prompt/driving text, the driving image, and the voice profile of an individual and then combines them to pass them to the multi-entangled latent space to foster key-value pairs and queries for the audio and video modality generation pipeline. The multi-entangled latent space is responsible for establishing the spatiotemporal person-specific features between the modalities. Further, entangled features are passed to the respective decoder of each modality for output audio and video generation. Our experiments and analysis through standard metrics demonstrate the effectiveness of our model. All model checkpoints, code, and the proposed dataset can be found at <https://github.com/narratingForYou/NarratingForYou>.

1. Introduction

AI-generated real-time audio-video multimedia communication by rendering realistic human talking faces has recently drawn massive attention [1, 2]. Such technology is promising in various applications such as digital communication, aiding communication with individuals with impairments, designing artificial instructors, and developing interactive healthcare [10, 39]. In such applications, generating realistic and real-time speech and visual content simultaneously is a key requirement. Therefore, in an ideal scenario, given a prompt text along with a face image and the audio profile of an individual, a talking human face would be rendered as output with audio (generated speech) and visual narration according to the prompt text.

Generative AI has emerged as a key area of interest in the computer vision, multimedia, learning representation, and machine learning community. Although existing approaches have made significant strides, they are constrained by their reliance on generating a single modality [9, 16]. For example, current text-to-speech models (TTSM) [3, 5, 7] focus primarily on voice synthesis. Similarly, visual generation techniques i.e. talking face models (TFM) [25, 26, 29, 39–41, 44] aim at face video generation given a text or/and audio or/and image as a prompt. Hence, both TTSM and TFM techniques are unsuitable for real-life audio-video multimedia communication scenarios such as audio-visual chatbots, as in such situations, both realistic video and speech must be generated synchronously and simultaneously. Few efforts have been made in the literature to merge TTSM and TFM by cascading the pipeline [37, 43]. Additionally, [13] made an effort to generate a talking face and speaking audio jointly for a specific individual from a prompt text. However, as the audio generation is not based on an audio prompt it is not generalized for real-life applications.

Further, these TFM [8, 45] depend on guidance from defined facial properties from the weakly supervised latent information from the reference modality. As a result, poor lip-synchronization and limited ability to tune an existing audio profile for personalizing the video content lead to a generation that is far from being realistic. Moreover, expressiveness in facial dynamics, along with subtle nuances for realistic facial behavior, needs to match simultaneously with audio content temporally to produce realistic talking faces. Further, such synchronization also depends on individual traits, such as speech intonation and other covariates. Although they are supposed to be important considerations for realistic speaking and talking faces models (STFM), However, this was not in the scope of existing work on STFM [13]. Therefore, this gap in the literature motivates us to design a prompt text-guided audio-visual multimodal generative STFM that can jointly generate audio and video, given a

*Equally contributing first authors.

†Corresponding author.

reference image and reference audio along with the prompt text as input.

Consequently, in contrast to existing literature, in this work, we introduce a novel multi-modal framework designed to address these limitations by generating highly realistic speech and animations from a combination of prompt text, a driving image, and an audio profile as inputs. Specifically, our framework aims to synthesize videos of a talking human face where the person in the image appears to speak along with the generated voice from the provided text for the given identity. Our method enhances the capabilities of existing pre-trained models [39] with an advanced parallel mechanism that leverages both visual and auditory data streams. This parallelism ensures that the synthesized videos not only align the subject’s facial movements with the spoken text but also synchronize with the generated personalized voice outputs that correspond to the subject’s appearance.

A person-agnostic generalized STFM model must encompass a large appearance and acoustic features variation. Furthermore, extracting such structure information along with the temporal synergy between the audio and video while preserving individual variance requires additional modules to model these complexities. Therefore, we introduce a parallel multiple entanglement in the latent space between the encoding and decoding of different modalities. The encoding stage is designed to generate structured representations that are enhanced in the latent space to generate the target representation in the decoding stage.

Our proposed architecture for STFM contains three main phases (See Figure 1). *Modality encoding phase*, at this stage a heterogeneous personal signature of the audio and video modality, and the driving feature from the text are extracted. The second stage is the *multi-entangled latent space* which glens the spatiotemporal relation and synchronization in the embeddings of the modalities, which further acts as the input to the *decoders phase* i.e the third stage of the proposed architecture. In the second stage, the exchange of information between the key and values (identity information from audio and video extracted from the individual encoders) and queries (driving features from encoded prompt text) are streamlined. To instrument this, an entanglement of the audio and text latent is performed, which further entangles with video latent in the transformer block and then to a diffusion block. The output of the diffusion block is passed to the video decoder. Similarly, an entanglement of the video and text latent is performed, which further entangles with audio latent in a transformer space and passes to a text decoder block and then to the audio decoder. Such entanglements ensure to streamlining of the audio profile and the driving image by linear navigation in the latent space along with the encoded feature from the

prompt text. Specifically, the temporal information for both the audio and video generation is constructed by linear displacement of codes in the latent space as per the encoded text prompt. In turn, the model also learns a set of orthogonal motion directions to simultaneously learn the audio and video temporal synergy by exchanging their linear combination to represent any displacement in the latent space. To summarize, our key contributions are as follows:

- To the best of our knowledge, the proposed architecture is the first person-agnostic STFM which fosters a text-driven multimodal realistic audio-video synthesis that can be generalized to any identity.
- We design a three-phase architecture which consists of the encoder, multi-entangled latent and decoder phase for audio and video pipeline. The multi-entangled latent space glens the spatiotemporal and synchronisation in the encoder embedding to exchange information between the modality and guided text and help to generate crucial visual and acoustic characteristics based on input profiles.
- With the comprehensive experiments, we demonstrate that the proposed method surpasses the state-of-the-art techniques available for STFM.

2. Related Work

Modern Text-To-Speech approaches as[5, 7], Tacitron[35] and the newer Tacitron2[28] are quite popular. The spectrograms generated from these models are then passed through neural vocoders like WaveNet[32] or HiFi-GAN[19] to generate high-quality audio waveforms. Other models, such as FastSpeech[24] and VITS[16], are noteworthy for improving the speed of speech generation. TortoiseTTS[5] is a modern, expressive TTS system with impressive voice cloning capabilities which incorporates a combination of the Auto-Regressive Model, followed by a Diffusion Model[11]. This model also follows the standard of a vocoder(Univnet)[12] for generating the audio from the spectrogram frames. Only a few works have been made in the literature to attend STFM by cascading the pipeline [37, 43]. In [13] advancements are made by generating a talking face and speaking audio jointly for a specific individual from a prompt text. Face reenactment and lip-sync models, such as SyncNet[23], focused on lip synchronisation through facial key points and phoneme mapping. More recent models, such as LipGAN[14] and Wav2Lip[21], leverage GANs to improve lip-sync accuracy. Diffusion-based lip-Sync models such as Audio2Head[34], Expressive Audio-driven Talking-heads (EAT)[10], Hallo[39], SadTalker[44], FaceChain ImagineID[38], Diffused Heads[31] and DreamTalk[41] have been proposed in the literature of TFM.

3. Proposed Architecture for STFM

We propose an architecture for STFM for joint learning methodology for the audio, video, and natural language-based text prompts consisting of three main components, namely, (1) Encoding phase, (2) Entanglement of combined latent space, and (3) Decoding phase *i.e.*, Latent conditional generation of synthesised audio-video. Figure 1 illustrates the detailed network architecture and roles of different model components to learn and dynamically synthesise audio and video on a given source image.

3.1. Multi-modal Encoding Phase.

The encoder stage aims to glean the heterogeneous personal signature and the coded latent form as per the length of the output sequence of the audio and video modality, along with the driving encoded feature from the text.

Hence, to encode the audio modality, two sets of encoders are employed. One set will encode the personal signature of the modality for the respective individual whose source image and reference audio are passed as input, and the second set of encoders features the input as per the length of the output sequence. For the audio sequence encoding \mathbf{E}_{AS} , we use the HiFi-GAN encoder [19], which takes a mel-spectrogram as input and upsamples it through transposed convolutions to the length of the output sequence as per the temporal resolution of raw waveforms. For the audio signature/profile encoding \mathbf{E}_{AP} , we employed Wav2Vec Encoder [4] to extract high-dimensional heterogeneous personal embedding vectors from the reference audio. The \mathbf{E}_{AS} generates a feature embedding \mathbf{f}_{AS} that represents the output sequence audio waveform. At the same time, the \mathbf{E}_{AP} produces a personal audio signature embedding \mathbf{f}_{AP} capturing semantic of individual specific audio information. Hence, the semantic audio embedding is a direct mapping of the speaker’s voice profile. Consequently, the combined features $\mathbf{f}_{AS} \oplus \mathbf{f}_{AP}$ provide a detailed feature \mathbf{f}_{ASP} as per the output sequence along with audio profile necessary for driving the audio generation. The input reference audio is represented as a 2-second MEL-spectrogram, encoder into a sequence of acoustic features per frame of 0.2 seconds duration with the shape of $\mathbb{R}^{5609 \times 512}$.

For the input text prompt is encoding by \mathbf{E}_T employing a Byte-Pair Encoding (BPE) and Tokenization [48] to convert textual information into a feature vector $\mathbf{f}_t \in \mathbb{R}^{512 \cdot T}$. This feature vector enables output context-specific information, allowing the synthesized video and audio to align with the intended spoken words and expressions implied in the text. To enable the audio feature vector with the output context a concatenating \mathbf{f}_t with the combined feature of reference audio $\mathbf{f}_{AS} \oplus \mathbf{f}_{AP}$ is to obtain the speaker’s signature in the final flattened feature tokens of $\mathbf{f}_t \oplus \mathbf{f}_{AS} \oplus \mathbf{f}_{AP} \in \mathbb{R}^{5609+T \times 512}$.

For a video sequence, two encoders are employed: a visual appearance encoder \mathbf{E}_{VA} and the visual structural en-

coding \mathbf{E}_{VS} to process the input source image. For \mathbf{E}_{VA} a Variational Auto-Encoder (VAE) [18] which encodes the appearance feature of the input and a landmarks detection model [42] for \mathbf{E}_{VS} which can capture the structural feature of the profile. The VAE generates an image embedding \mathbf{f}_i , representing the visual style and identity of the person in the source image. Concurrently, the landmarks detection network extracts structural features face mask feature \mathbf{f}_{fm} and lip mask feature \mathbf{f}_{lm} , which are combined with the image embedding vectors to create a fused visual feature representation $\mathbf{f}_i \oplus \mathbf{f}_{lm} \oplus \mathbf{f}_{fm} \in \mathbb{R}^{3136 \times 512}$. The straightforward tendency of traditional methods is either to introduce prior 3D morphable models faces [44], motion priors of the facial parts [13], or guiding video frames [36] to learn nuances of facial articulation concerning the audio in the combined latent space. In contrast, we show that the entanglement of multiple latent spaces of text-audio-video using Transformer encoders [33] can eliminate the dependency on strong motion priors. As a result, we are able to use text prompt features as a set of anchoring tokens to both the Transformer encoders. To enable the visual feature vector with the output context, a concatenation \mathbf{f}_t with the combined feature of reference visual feature $\mathbf{f}_i \oplus \mathbf{f}_{lm} \oplus \mathbf{f}_{fm}$.

3.2. Entanglement of Multi-modal Latent Space

As illustrated in Figure 1, a smooth synergy between the text-audio latent embedding and the text-image latent embedding is established by two Transformer encoders followed by a latent diffusion-guided [39] synthesiser of visual nuances and decoder employing GPT-2 decoder [7] to model text-conditioned of the audio latent.

The first Transformer encoder spatially contextualizes the audio MEL-spectrogram tokens using a dual-stream cross-modal attention (CA) mechanism with the flattened version, denoted by $\mathbf{L}(\cdot)$, of *categorically fixed speaker* embedding tokens merged with varying text embedding tokens, *i.e.*, $\mathbf{Q}_a = \mathbf{L}(\mathbf{f}_{AS} \oplus \mathbf{f}_{AP})$, as

$$\text{CA}(\mathbf{Q}_a, \mathbf{K}_{ti}, \mathbf{V}_{ti}) = \text{SoftMax} \left(\frac{\mathbf{Q}_a \mathbf{K}_{ti}^\top}{\sqrt{d_k}} \right) \mathbf{V}_{ti}, \quad (1)$$

where the query vector \mathbf{Q}_a is of dimension $\mathbb{R}^{5609 \times 512}$ and the key-value pairing $(\mathbf{K}_{ti}, \mathbf{V}_{ti})$ between the tokens of $\mathbf{L}(\mathbf{f}_t \oplus \mathbf{f}_i \oplus \mathbf{f}_{lm} \oplus \mathbf{f}_{fm})$ has a variable spatial length (padded up-to a max length) with a fixed channel length of 512. Merging the varying text tokens serves two purposes – (1) first, querying audio tokens as well as the speaker tokens has been implicitly prompt-engineered by the text tokens, (2) second, when the resulting prompt-engineered latent embedding vectors \mathbf{f}_{as} are split into their respective constituents, they become proxy weights of text-image embedding vectors.

Similar to the previous encoder block, the second Transformer encoder spatially contextualizes the input masked-

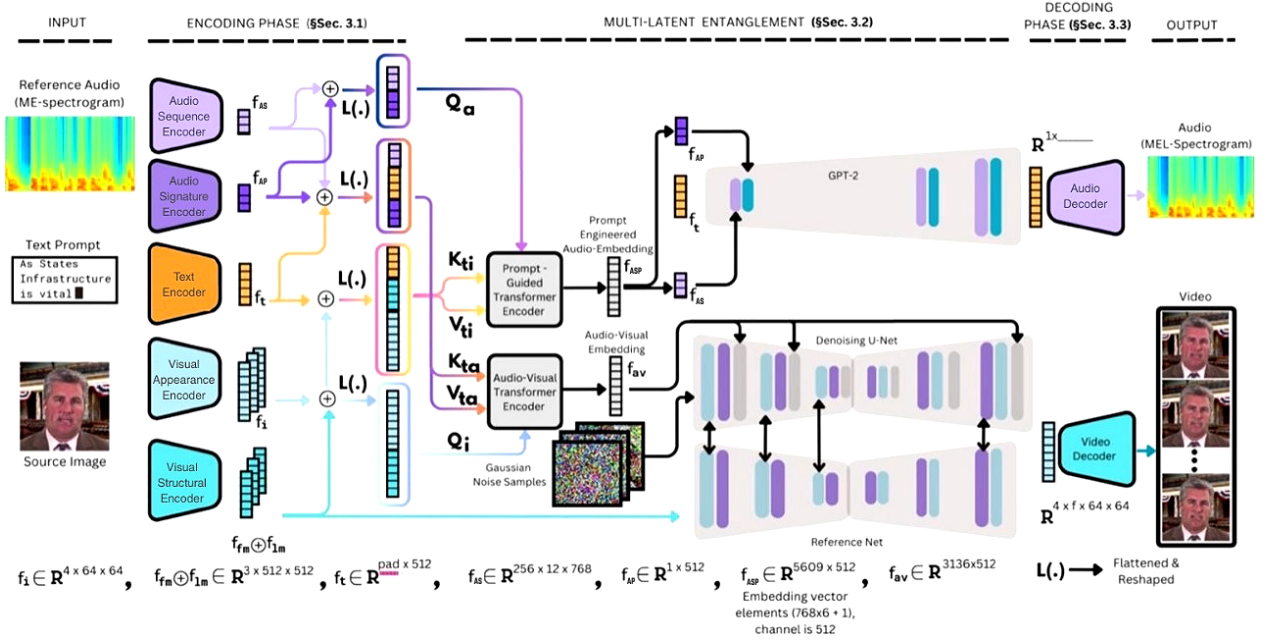


Figure 1. **Our Network Architecture:** Text Prompt-guided joint audio-visual learning representations using dual stream Transformer Encoders and Denoising Diffusion model. The model architecture can be divided into three phases – namely *Encoding Phase*, *Multi-Latent Entanglement*, and *Decoding Phase*. As an output, an audio-visual animation is generated from a single source image, reference audio, and a short text prompt.

image embedding vectors $L(f_i \oplus f_{fm} \oplus f_{lm})$ using cross-modal attention (CA) with the key-value pairs (K_{ta} , V_{ta}) of merged text-audio embedding tokens $L(f_t \oplus f_{AS} \oplus f_{AP})$ similar to the (1) as

$$CA(Q_i, K_{ta}, V_{ta}) = \text{SoftMax} \left(\frac{Q_i K_{ta}^\top}{\sqrt{d_k}} \right) V_{ta}. \quad (2)$$

As a result, the output latent embedding on audio-visual features f_{av} can serve as a compact and compressed representation of facial animation sequences in the high-dimensional space. Therefore, our next step is to learn a synthesizer *i.e.*, a hierarchical latent diffusion model [39] for video generation and a corresponding MEL-spectrogram synthesizer based on the X-Text-to-Speech (XTTS) model [7].

Latent Text Conditioned Spectrogram Synthesizer: The GPT-2 encoder is based on the TTS model [6] and [28]. This part is composed of a decoder-only transformer module that is conditioned by the audio and speaker embedding vectors f_{AS} , f_{AP} disentangled from the prompt-engineered audio embedding vector f_{av} , and the autoregressive generation of spectrogram tokens is fully driven by the input text tokens from f_{av} .

Text-Anchored Audio-Video Latent Conditioned Denoising Diffusion: The Denoising Diffusion model aims to reverse a diffusion process [11, 30] that progressively adds random Gaussian noise to data. Additionally, we employ an

augmentation of the text-anchored latent embedding vector, learned to combine the audio and motion nuances within a single image, inside the Denoising U-Net [27].

Throughout each step of the diffusion process, we introduce embedding cross-attention, which incorporates the combined latent space embedding, particularly our f_{av} , into each diffusion step. This cross-attention mechanism allows the diffusion models to leverage the shared information across modalities, ensuring that the generated outputs (audio and video) are consistent with the input embedding. The inclusion of cross-attention helps to maintain coherence between the synthesised motion across all the pixels of the source image.

Additionally, diffusion cross-attention facilitates mutual information exchange between the audio and video diffusion blocks. This cross-attention mechanism enables the audio and video models to synchronise their outputs, ensuring that the generated audio and video components are temporally aligned. By integrating this cross-attention, our framework effectively coordinates the diffusion processes, leading to synchronised and coherent multimedia output.

3.3. Decoding Phase for Audio-Video Generation

The outputs of the previous steps are processed by their respective final decoders. For audio generation, the synthesised spectrogram is passed through a Vocoder component of HiFi Generator module to obtain the final audio sig-

nal. For video, the Denoising UNet generates f number of frames of dimension $\mathbb{R}^{4 \times f \times 64 \times 64}$, which are decoded by a pre-trained decoder component of [17] to produce the complete video.

3.4. Loss Functions

To train our model, we used (1) Video Loss as the Pixel-wise L1 Loss *i.e.*, sum of the N number of pixel intensities between the ground truth image frame $\mathcal{I}_{\text{gt}}^f$ and the generated frame $\mathcal{I}_{\text{gen}}^f$ for all the f number of frames as $\mathcal{L}_{\text{video}} = \sum_f \sum_{i=1}^N \|(\mathcal{I}_{\text{gt}}^f)^i - (\mathcal{I}_{\text{gen}}^f)^i\|$, (2) Audio Loss as the Spectrogram MSE loss at the spectrogram \mathcal{S} domain as mean squared error between the ground-truth magnitudes and generated magnitudes at different of time step t as $\mathcal{S}_{\text{gt}}^t$ and the generated frame $\mathcal{S}_{\text{gen}}^t$ as $\mathcal{L}_{\text{audio}} = \frac{1}{T} \sum_{t \in T} \|(\mathcal{I}_{\text{gt}}^f)^i - (\mathcal{I}_{\text{gen}}^f)^i\|^2$. Total loss as $\mathcal{L}_{\text{Total}} = \lambda \mathcal{L}_{\text{audio}} + \mathcal{L}_{\text{video}}$ with regulations factor $\lambda = 0.1$.

4. Experimental Results

4.1. Datasets, Implementation and Evaluation

Datasets: We have primarily conducted our experiments on 4 datasets. Our model training was done on a combination of **VoxCeleb** Dataset [20], **FakeAVCeleb** dataset [15], **HDTF** [46] and the **CelebV-HQ** dataset [47]. For our experiment, we developed a subset of this dataset with 36000 videos. We chose this training set by filtering out individuals whose speech was in English from four datasets (VoxCeleb, FakeAVCeleb, CelebV-Hq and HDTF). The text transcribing was done using the Whisper model by OpenAI. For the source image, we just took the first frame of the video, and for the audio profile, we trimmed down the audio we extracted from the video to 2 seconds. We tested on more than 200 samples from each of the 4 datasets, resulting in a test set of over 800 unseen samples.

Preprocessing: Our preprocessing involved resizing the videos to 512x512 and then cropping each video sample to the first 20 seconds (at 25FPS which equates to 500 frames). We then separated the audio from the video using ffmpeg, and then ran the OpenAI’s Whisper model[22] to transcribe the audio speeches.

Implementation details: The optimizer used for our model is AdamW with a learning rate of 1e-4 and weight decay of 1e-2, and the scheduler has a step-wise learning rate with a step size of 1000 and gamma of 0.5. The weight decay regularises the model, preventing any overfitting. We have used Nvidia 1xA6000s GPUs for training each model, and the model inference requires 12GB of VRAM. The total parameter size of the model comes to 1,575,936 and performs 5.39 GFLOPs (Giga Floating Point Operations) per generation. We have trained the models for 10 epochs, with a batch size of 8. The Hifi-Gan, Wav2Vec Encoders, the Variational Autoencoder, Diffusion Models, and the GPT2

Decoder were pre-trained which were further trained with the rest of the entire proposed network.

Evaluation Metrics: Following are the evaluation matrices employed. For video generation, Fréchet Video Distance (FVD), Fréchet Inception Distance (FID), Fréchet Video Motion Distance(FVMD), Peak Signal-to-Noise Ratio (PSNR), Structural Similarity Index (SSIM), Kernel Video Distance (KVD), Learned Perceptual Image Patch Similarity (LPIPS) and Mean Opinion Score (MOS) were also employed. For the MOS score, we involved 35 human experts, who scored the video and audio in range of 0-5. Metrics such as Fréchet Audio Distance (FAD), Short-Time Objective Intelligibility (STOI), Mel Cepstral Distortion(MCD), Word Error Rate (WER), Extended STOI (ES-TOI), Perceptual Evaluation of Speech Quality (PESQ) and MOS were used. For AV synchronisation, Lip Sync Error Distance (LSE-D) and Lip Sync Error Confidence (LSE-C) were employed.

4.2. Result Analysis

Video Results: From Table 1 and Table 2, we can observe that our model shows superior performance across all metrics employed on VoxCeleb, CelebV-Hq and HDTF. This indicates high fidelity and that minimal discrepancies are addressed by the proposed model. On the FakeAVCeleb, the performance is slightly poorer but can be comparable; it still maintains strong visual consistency and realism on visual inspection. For the CelebV-HQ, our model excels again, demonstrating its capability to produce high-quality video outputs. On HDTF, our model shows incredible performance in the FID and FVD metrics, beating all the other models, while our model is admirably performing considering FVMD when compared to Hallo.

Based on the results, we observed that for some datasets, certain models work slightly better than the proposed model, and the reason behind this is that those models try to memorise certain properties from individual datasets. Whereas our model is a more generalized version that can be performed consistently on cross-datasets having varying resolution and video quality. The visualisation from Figure 2 also concludes that our model can generate video very close to the ground truth and better than any model. From Figure 3 it can be concluded that our model can generate nearby results for HDTF, FakeAVCeleb and CelebV-HQ when compared to the ground truth.

Audio Results: We can infer from Table 3 and Table 4 that our model consistently performs the best in considering all measures. The MCD Score metric suggests that it minimizes distortion between the spectral features of synthetic and reference speech. While considering the FAD scores, our model also performed on par with state-of-the-art, except on VoxCeleb where Your_TTS is better; these showcase that the proposed model can generate consistently sim-

Table 1. Video pipeline evaluation scores across datasets.

Dataset	Model	FID (\downarrow)	FVD (\downarrow)	FVMD (\downarrow)
VoxCeleb	Audio2Head	81.00	90.12	5100.92
	Hallo	67.28	70.69	5703.44
	EAT	85.16	80.38	4878.36
	SadTalker	119.36	112.77	6352.19
	Our Model	42.88	49.78	4192.07
FakeAVCeleb	Audio2Head	93.59	97.85	1329.23
	Hallo	26.88	39.42	2351.20
	EAT	94.34	98.49	1324.91
	SadTalker	81.77	77.10	4158.18
	Our Model	47.24	49.15	2263.54
CelebV-HQ	Audio2Head	90.22	102.76	2939.49
	Hallo	42.76	56.10	2816.68
	EAT	47.88	56.21	2894.31
	SadTalker	52.60	52.55	2789.19
	Our Model	34.01	43.67	2743.29
HDTF	Audio2Head	37.78	32.69	2633.04
	Hallo	20.54	25.81	1290.57
	EAT	29.57	29.34	2573.05
	SadTalker	22.34	23.57	2410.89
	Our Model	11.72	15.58	1784.16

Table 2. Evaluation of video quality metrics.

Method	PSNR (\uparrow)	SSIM (\uparrow)	KVD (\downarrow)	LPIPS (\downarrow)	MOS (\uparrow)
Hallo	33.01	0.68	44.12	0.51	4.10
Audio2Head	29.21	0.51	49.09	0.23	3.51
EAT	24.45	0.52	49.12	0.52	3.57
SadTalker	29.72	0.59	49.61	0.53	3.51
Proposed	35.94	0.73	41.22	0.54	4.22

ilar audio compared to the ground truth. Considering the STOI metric, the performance of our model is similar to or slightly lower than Your_TTS. The analysis of all the measures showcases that our model is more generalized and realistic as it can minimise distortion and also generate accurate distributions, and maintain intelligibility of the speech consistently better than any other models. The visualization from Figure 4 also concludes that our model can generate audio very close to the ground truth.

AV synchronisation results: From Table 5, we can conclude that our proposed model has performed better audio-video synchronization than SOTA and is close to the ground truth. The proposed model has the lowest LSE-D, i.e. better audio-visual match, i.e. and LSE-C i.e. better audio-video correlation. We have also analysed the model with varying accents, blurred audio profiles, and audio profiles of a kid with a source image of an adult and vice versa, and the results were found to be very effective; no bias was found in any aspect. Models fail in a few scenarios where a very noisy audio profile is used, output audio is feeble or for

Table 3. Audio pipeline evaluation scores across datasets.

Dataset	Model	FAD (\downarrow)	MCD (\downarrow)	STOI (\uparrow)
VoxCeleb	Tortoise	258.54	82.37	0.10
	Your_TTS	199.52	111.79	0.19
	XTTS_v2	249.17	100.80	0.13
	GlowTTS	329.21	103.94	0.15
	Our Model	241.75	75.39	0.17
FakeAVCeleb	Tortoise	871.14	82.12	0.10
	Your_TTS	445.38	65.60	0.21
	XTTS_v2	184.39	77.88	0.11
	GlowTTS	482.04	87.11	0.18
	Our Model	171.52	55.12	0.19
CelebV-HQ	Tortoise	529.06	113.18	0.09
	Your_TTS	520.01	137.58	0.16
	XTTS_v2	509.90	124.61	0.07
	GlowTTS	549.18	139.81	0.22
	Our Model	244.83	85.76	0.18
HDTF	Tortoise	425.30	67.15	0.11
	Your_TTS	467.42	49.38	0.15
	XTTS_v2	135.11	49.65	0.14
	GlowTTS	510.61	66.42	0.12
	Our Model	106.43	44.05	0.15

Table 4. Evaluation of audio quality metrics.

Method	ESTOI (\uparrow)	PESQ (\uparrow)	WER (\downarrow)	MOS (\uparrow)
Tortoise	0.42	3.80	0.21	4.32
Your_TTS	0.31	3.71	0.30	3.61
XTTS_v2	0.33	3.51	0.34	3.21
GlowTTS	0.39	3.83	0.33	3.52
Proposed	0.43	4.01	0.18	4.56

Table 5. Evaluation of audio-visual synchronisation.

Model	LSE-C (\uparrow)	LSE-D (\downarrow)
Groundtruth	5.45	8.52
Hallo	3.03	8.71
Audio2Head	2.51	10.34
EAT	4.39	9.35
SadTalker	5.44	10.09
STE	5.71	8.41
ETE/Proposed	5.74	8.38

source images with closed eyes, face dynamics get affected.

4.3. Ablation Study

Table 6 shows the ablation study of our proposed model. We have 3 main sub-networks that define the output of our model. The **Transformer Encoder Block(TE)** [33] with two variations shared-TE (**STE**), where both audio and video pipeline share a transformer block and explicit-TE (**ETE**) where audio and video pipeline have explicit

Table 6. Ablation study of the transformer and cross-attention components. **STE**: Shared-TE, **ETE**: Explicit-TE, **DC**: Diffusion Cross-Attention, **EC**: Embedding Cross-Attention.

Components				Video Metrics			Audio Metrics		
ETE	STE	DC	EC	FID (↓)	FVD (↓)	FVMD (↓)	FAD (↓)	MCD (↓)	STOI (↑)
		✓	✓	86.70	80.88	5275.89	328.27	95.44	0.07
	✓			68.83	74.19	4412.74	260.91	87.51	0.11
	✓	✓		63.68	71.38	4298.30	250.12	83.96	0.14
	✓	✓	✓	61.44	69.15	2720.41	241.77	81.60	0.17
✓		✓	✓	42.88	49.78	4192.07	241.75	75.39	0.17

Table 7. Ablation study of the encoder components.

Ablation Setting	FID (↓)	FVD (↓)	FVMD (↓)	FAD (↓)	MCD (↓)	STOI (↑)
Only Visual Tokens Attended	68.31	78.42	5747.04	304.98	81.17	0.13
Only Audio Tokens Attended	69.02	79.35	6576.85	301.49	80.65	0.13
No audio sequence encoding	85.25	94.28	7483.40	498.33	87.51	0.09
No audio profile encoding	70.10	80.96	5926.64	309.95	89.58	0.11
No visual token encoding	54.38	62.02	5481.36	221.07	63.25	0.12
Proposed Model	42.88	49.78	4192.07	241.75	75.39	0.17

or separate transformer blocks. **Diffusion[30] Cross Attention(DC)**, and the **Embedding Cross Attention(EC)**. From our results, it is understandable and explainable that the transformer encoder block, which encodes our inputs into a common latent space, is the most important modality of our network, with its removal drastically reducing our metric values. Our experiments also show that the cross-attention blocks between the diffusion models are more important than the embedding cross-attention, since our metric values drop more when we remove the diffusion cross-attention, probably since the diffusion cross-attention already syncs the modalities during the parallel learning stage. Another important aspect of ablation is the encoding latent in the individual transformer i.e. ETE is much better than STE. This implies that it is important to encode the latent for each modality separately while sharing information among the generated modalities.

Table 7 shows our ablation study on the encoders. “Only Visual Tokens Attended” involves eliminating the audio prompt-guided transformer. Similarly, the “Only Audio Tokens Attended” involves using only the audio prompt-guided transformer. “No-audio sequence encoding” and “No audio profile encoding” are results obtained by eliminating the encoding process of the Hifi-GAN and Wav2Vec models, respectively. “No Visual token in prompt-guided-Transformer” involves not attending to the visual tokens in the prompt-guided-Transformer.

4.4. Social Risks and Mitigations

There are social risks with technology development for text-driven audio-video talking face generation in regards to pri-

vacy, malicious acts, etc. To mitigate such risk, ethical guidance for the use of such generation techniques is required. By addressing these, we aim to promote responsible and ethical generative technology.

5. Conclusion

This paper introduces a novel method for realistic speaking and talking faces by joint multimodal video and audio generation. We provide a holistic architecture where the information is exchanged between the modalities via the proposed multi-entangled latent space. A source image of an individual as a driving frame, reference audio, which can be referred to as the audio profile of the individual and a driving or prompt text is passed as an input. The model encodes the input driving image, prompt/driving text, and the voice profile, which are further combined and passed to the proposed multi-entangled latent space consisting of two separate transformers and a diffusion block for video and text decoder for audio pipeline to foster key-value and query representation for each modality. By this spatiotemporal person-specific features between the modalities are also established. The entangled-based learning representation is further passed to the respective decoder of audio and video modality for respective outputs. Conducted experiments and ablation studies prove that the proposed multi-entangled latent-based learning representation has helped our model obtain superior results on both video and audio outputs as compared to state-of-the-art models. While there is always scope for improvement in the future, we believe that our model has shown a promising new learning repre-



Figure 2. Visual comparison on VoxCeleb, in the order: Ground Truth, Ours, Audio2Head, EAT, Hallo, and SadTalker. Columns represent 25s intervals.

sensation for realistic speaking and talking face generation models.

Acknowledgements

This work was funded by the BITS Pilani-funded New Faculty Seed Grant (NFSG) under the project titled “Playing God-generation of virtual environment through masked auto-encoders and diffusion technique” and project number NFSG/HYD/2023/H0831.



Figure 3. Results of our model on FakeAVCeleb, CelebV-HQ and HDTF datasets.

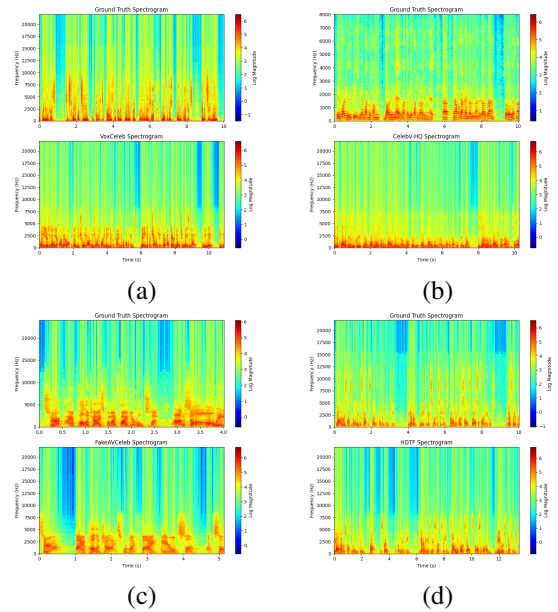


Figure 4. Ground Truth vs. Generated Audio Spectrograms for (a) VoxCeleb, (b) CelebV-HQ, (c) FakeAVCeleb and (d) HDTF datasets

References

- [1] <https://www.business-standard.com/technology/tech-news/odisha-television-introduces-lisa-india-s-first-ai-news->

- presenter-123071000767_1.html. 1
- [2] <https://www.indiatoday.in/india/story/india-today-groups-ai-anchor-sana-wins-global-media-award-for-ai-led-newsroom-transformation-2532514-2024-04-27>. 1
- [3] Junyi Ao, Rui Wang, Long Zhou, Chengyi Wang, Shuo Ren, Yu Wu, Shujie Liu, Tom Ko, Qing Li, Yu Zhang, Zhihua Wei, Yao Qian, Jinyu Li, and Furu Wei. Speech5: Unified-modal encoder-decoder pre-training for spoken language processing, 2022. 1
- [4] Alexei Baevski, Henry Zhou, Abdelrahman Mohamed, and Michael Auli. wav2vec 2.0: A framework for self-supervised learning of speech representations, 2020. 3
- [5] James Betker. Tortoise text-to-speech, 2022. Accessed: [date you accessed the repository]. 1, 2
- [6] Edresson Casanova, Julian Weber, Christopher Shulby, Arnaldo Candido Junior, Eren Gölge, and Moacir Antonelli Ponti. Yourtts: Towards zero-shot multi-speaker tts and zero-shot voice conversion for everyone, 2023. 4
- [7] Edresson Casanova, Kelly Davis, Eren Gölge, Görkem Gökner, Iulian Gulea, Logan Hart, Aya Aljafari, Joshua Meyer, Reuben Morais, Samuel Olayemi, and Julian Weber. Xtts: a massively multilingual zero-shot text-to-speech model, 2024. 1, 2, 3, 4
- [8] Ken Chen, Sachith Seneviratne, Wei Wang, Dongting Hu, Sanjay Saha, Md. Tarek Hasan, Sanka Rasnayaka, Tamasha Malepathirana, Mingming Gong, and Saman Halgamuge. Anifacediff: High-fidelity face reenactment via facial parametric conditioned diffusion models, 2024. 1
- [9] Bernhard Egger, William A. P. Smith, Ayush Tewari, Stefanie Wuhler, Michael Zollhoefer, Thabo Beeler, Florian Bernard, Timo Bolkart, Adam Kortylewski, Sami Romdhani, Christian Theobalt, Volker Blanz, and Thomas Vetter. 3d morphable face models – past, present and future, 2020. 1
- [10] Yuan Gan, Zongxin Yang, Xihang Yue, Lingyun Sun, and Yi Yang. Efficient emotional adaptation for audio-driven talking-head generation, 2023. 1, 2
- [11] Jonathan Ho, Ajay Jain, and Pieter Abbeel. Denoising diffusion probabilistic models, 2020. 2, 4
- [12] Won Jang, Dan Lim, Jaesam Yoon, Bongwan Kim, and Juntae Kim. Univnet: A neural vocoder with multi-resolution spectrogram discriminators for high-fidelity waveform generation, 2021. 2
- [13] Youngjoon Jang, Ji-Hoon Kim, Junseok Ahn, Doyeop Kwak, Hong-Sun Yang, Yoon-Cheol Ju, Il-Hwan Kim, Byeong-Yeol Kim, and Joon Son Chung. Faces that speak: Jointly synthesising talking face and speech from text. In *Proceedings of the IEEE/CVF Conference on Computer Vision and Pattern Recognition*, pages 8818–8828, 2024. 1, 2, 3
- [14] Prajwal K R, Rudrabha Mukhopadhyay, Jerin Philip, Abhishek Jha, Vinay Namboodiri, and C V Jawahar. Towards automatic face-to-face translation. In *Proceedings of the 27th ACM International Conference on Multimedia*. ACM, 2019. 2
- [15] Hasam Khalid, Shahroz Tariq, Minha Kim, and Simon S. Woo. Fakeavceleb: A novel audio-video multimodal deepfake dataset, 2022. 5
- [16] Jaehyeon Kim, Jungil Kong, and Juhee Son. Conditional variational autoencoder with adversarial learning for end-to-end text-to-speech, 2021. 1, 2
- [17] Diederik P. Kingma and Max Welling. An introduction to variational autoencoders. *Foundations and Trends® in Machine Learning*, 12(4):307–392, 2019. 5
- [18] Diederik P Kingma and Max Welling. Auto-encoding variational bayes, 2022. 3
- [19] Jungil Kong, Jaehyeon Kim, and Jaekyoung Bae. Hifi-gan: Generative adversarial networks for efficient and high fidelity speech synthesis, 2020. 2, 3
- [20] Arsha Nagrani, Joon Son Chung, Weidi Xie, and Andrew Senior. Voxceleb: Large-scale speaker verification in the wild. *Computer Science and Language*, 2019. 5
- [21] K R Prajwal, Rudrabha Mukhopadhyay, Vinay P. Namboodiri, and C.V. Jawahar. A lip sync expert is all you need for speech to lip generation in the wild. In *Proceedings of the 28th ACM International Conference on Multimedia*. ACM, 2020. 2
- [22] Alec Radford, Jong Wook Kim, Tao Xu, Greg Brockman, Christine McLeavey, and Ilya Sutskever. Robust speech recognition via large-scale weak supervision, 2022. 5
- [23] Akshay Raina and Vipul Arora. Syncnet: Using causal convolutions and correlating objective for time delay estimation in audio signals, 2022. 2
- [24] Yi Ren, Yangjun Ruan, Xu Tan, Tao Qin, Sheng Zhao, Zhou Zhao, and Tie-Yan Liu. FastSpeech: Fast, robust and controllable text to speech, 2019. 2
- [25] Yurui Ren, Ge Li, Yuanqi Chen, Thomas H. Li, and Shan Liu. Pirenderer: Controllable portrait image generation via semantic neural rendering, 2021. 1
- [26] Robin Rombach, Andreas Blattmann, Dominik Lorenz, Patrick Esser, and Björn Ommer. High-resolution image synthesis with latent diffusion models, 2022. 1
- [27] Olaf Ronneberger, Philipp Fischer, and Thomas Brox. U-net: Convolutional networks for biomedical image segmentation, 2015. 4
- [28] Jonathan Shen, Ruoming Pang, Ron J. Weiss, Mike Schuster, Navdeep Jaitly, Zongheng Yang, Zhifeng Chen, Yu Zhang, Yuxuan Wang, RJ Skerry-Ryan, Rif A. Saurous, Yannis Agiomyriannakis, and Yonghui Wu. Natural tts synthesis by conditioning wavenet on mel spectrogram predictions, 2018. 2, 4
- [29] Aliaksandr Siarohin, Stéphane Lathuilière, Sergey Tulyakov, Elisa Ricci, and Nicu Sebe. First order motion model for image animation, 2020. 1
- [30] Jiaming Song, Chenlin Meng, and Stefano Ermon. Denoising diffusion implicit models, 2022. 4, 7
- [31] Michał Stypułkowski, Konstantinos Vougioukas, Sen He, Maciej Zięba, Stavros Petridis, and Maja Pantic. Diffused heads: Diffusion models beat gans on talking-face generation, 2023. 2
- [32] Aaron van den Oord, Sander Dieleman, Heiga Zen, Karen Simonyan, Oriol Vinyals, Alex Graves, Nal Kalchbrenner, Andrew Senior, and Koray Kavukcuoglu. Wavenet: A generative model for raw audio, 2016. 2

- [33] Ashish Vaswani, Noam Shazeer, Niki Parmar, Jakob Uszkoreit, Llion Jones, Aidan N. Gomez, Lukasz Kaiser, and Illia Polosukhin. Attention is all you need, 2023. 3, 6
- [34] Suzhen Wang, Lincheng Li, Yu Ding, Changjie Fan, and Xin Yu. Audio2head: Audio-driven one-shot talking-head generation with natural head motion, 2021. 2
- [35] Yuxuan Wang, RJ Skerry-Ryan, Daisy Stanton, Yonghui Wu, Ron J. Weiss, Navdeep Jaitly, Zongheng Yang, Ying Xiao, Zhifeng Chen, Samy Bengio, Quoc Le, Yannis Agiomyriannakis, Rob Clark, and Rif A. Saurous. Tacotron: Towards end-to-end speech synthesis, 2017. 2
- [36] Yaohui Wang, Di Yang, Francois Bremond, and Antitza Dantcheva. Latent image animator: Learning to animate images via latent space navigation. *arXiv preprint arXiv:2203.09043*, 2022. 3
- [37] Zhichao Wang, Mengyu Dai, and Keld Lundgaard. Text-to-video: a two-stage framework for zero-shot identity-agnostic talking-head generation. *arXiv preprint arXiv:2308.06457*, 2023. 1, 2
- [38] Chao Xu, Yang Liu, Jiazheng Xing, Weida Wang, Mingze Sun, Jun Dan, Tianxin Huang, Siyuan Li, Zhi-Qi Cheng, Ying Tai, and Baigui Sun. Facechain-agineid: Freely crafting high-fidelity diverse talking faces from disentangled audio, 2024. 2
- [39] Mingwang Xu, Hui Li, Qingkun Su, Hanlin Shang, Liwei Zhang, Ce Liu, Jingdong Wang, Yao Yao, and Siyu Zhu. Hallo: Hierarchical audio-driven visual synthesis for portrait image animation, 2024. 1, 2, 3, 4
- [40] Sicheng Xu, Guojun Chen, Yu-Xiao Guo, Jiaolong Yang, Chong Li, Zhenyu Zang, Yizhong Zhang, Xin Tong, and Baining Guo. Vasa-1: Lifelike audio-driven talking faces generated in real time, 2024.
- [41] Chenxu Zhang, Chao Wang, Jianfeng Zhang, Hongyi Xu, Guoxian Song, You Xie, Linjie Luo, Yapeng Tian, Xiaohu Guo, and Jiashi Feng. Dream-talk: Diffusion-based realistic emotional audio-driven method for single image talking face generation, 2023. 1, 2
- [42] Fan Zhang, Valentin Bazarevsky, Andrey Vakunov, Andrei Tkachenka, George Sung, Chuo-Ling Chang, and Matthias Grundmann. Mediapipe hands: On-device real-time hand tracking, 2020. 3
- [43] Sibozhang, Jiahong Yuan, Miao Liao, and Liangjun Zhang. Text2video: Text-driven talking-head video synthesis with personalized phoneme-pose dictionary. In *ICASSP 2022-2022 IEEE International Conference on Acoustics, Speech and Signal Processing (ICASSP)*, pages 2659–2663. IEEE, 2022. 1, 2
- [44] Wenxuan Zhang, Xiaodong Cun, Xuan Wang, Yong Zhang, Xi Shen, Yu Guo, Ying Shan, and Fei Wang. Sadtalker: Learning realistic 3d motion coefficients for stylized audio-driven single image talking face animation, 2023. 1, 2, 3
- [45] Yunxuan Zhang, Siwei Zhang, Yue He, Cheng Li, Chen Change Loy, and Ziwei Liu. One-shot face reenactment, 2019. 1
- [46] Zhimeng Zhang, Lincheng Li, Yu Ding, and Changjie Fan. Flow-guided one-shot talking face generation with a high-resolution audio-visual dataset. In *Proceedings of the IEEE/CVF Conference on Computer Vision and Pattern Recognition*, pages 3661–3670, 2021. 5
- [47] Hao Zhu, Wayne Wu, Wentao Zhu, Liming Jiang, Siwei Tang, Li Zhang, Ziwei Liu, and Chen Change Loy. Celebv-hq: A large-scale video facial attributes dataset, 2022. 5
- [48] Vilém Zouhar, Clara Meister, Juan Luis Gastaldi, Li Du, Tim Vieira, Mrinmaya Sachan, and Ryan Cotterell. A formal perspective on byte-pair encoding, 2024. 3